(12) INTERNATIONAL APPLICATION PUBLISHED UNDER THE PATENT COOPERATION TREATY (PCT)

(19) World Intellectual Property Organization
International Bureau

(43) International Publication Date
1 April 2010 (01.04.2010)

PCT

(10) International Publication Number
WO 2010/035035 A2

(51) International Patent Classification:
B81B 1/00 (2006.01)

(21) International Application Number:
PCT/GB2009/051246

(22) International Filing Date:
24 September 2009 (24.09.2009)

(25) Filing Language: English

(26) Publication Language: English

(30) Priority Data:
0817519.2 24 September 2008 (24.09.2008) GB

(71) Applicant *(for all designated States except US)*: **CAMBRIDGE ENTERPRISE LIMITED** [GB/GB]; The Old Schools, Trinity Lane, Cambridge, Cambridgeshire CB2 1TN (GB).

(72) Inventors; and

(75) Inventors/Applicants *(for US only)*: **SCOTT, James Floyd** [US/GB]; Thorndyke, Huntingdon Road, Cambridge, Cambridgeshire CB3 0LG (GB). **FAN, Hongjin** [CN/SG]; 96 Nanyang Crescent, #02-11, Singapore 637664 (SG).

(74) Agent: **GILL JENNINGS & EVERY LLP**; Broadgate House, 7 Eldon Street, London EC2M 7LH (GB).

(81) Designated States *(unless otherwise indicated, for every kind of national protection available)*: AE, AG, AL, AM, AO, AT, AU, AZ, BA, BB, BG, BH, BR, BW, BY, BZ, CA, CH, CL, CN, CO, CR, CU, CZ, DE, DK, DM, DO, DZ, EC, EE, EG, ES, FI, GB, GD, GE, GH, GM, GT, HN, HR, HU, ID, IL, IN, IS, JP, KE, KG, KM, KN, KP, KR, KZ, LA, LC, LK, LR, LS, LT, LU, LY, MA, MD, ME, MG, MK, MN, MW, MX, MY, MZ, NA, NG, NI, NO, NZ, OM, PE, PG, PH, PL, PT, RO, RS, RU, SC, SD, SE, SG, SK, SL, SM, ST, SV, SY, TJ, TM, TN, TR, TT, TZ, UA, UG, US, UZ, VC, VN, ZA, ZM, ZW.

(84) Designated States *(unless otherwise indicated, for every kind of regional protection available)*: ARIPO (BW, GH, GM, KE, LS, MW, MZ, NA, SD, SL, SZ, TZ, UG, ZM, ZW), Eurasian (AM, AZ, BY, KG, KZ, MD, RU, TJ, TM), European (AT, BE, BG, CH, CY, CZ, DE, DK, EE, ES, FI, FR, GB, GR, HR, HU, IE, IS, IT, LT, LU, LV, MC, MK, MT, NL, NO, PL, PT, RO, SE, SI, SK, SM, TR), OAPI (BF, BJ, CF, CG, CI, CM, GA, GN, GQ, GW, ML, MR, NE, SN, TD, TG).

Published:

— *without international search report and to be republished upon receipt of that report (Rule 48.2(g))*

WO 2010/035035 A2

(54) Title: MICROTUBE ARRAYS

(57) Abstract: An array of microtubes upwardly extending from a supporting base of substrate material is provided, in which the tubes comprise at least one concentric layer comprising a metallic oxide and at least one concentric layer comprising a piezoelectric and/or ferroelectric material. The array is made by lining the walls of pores in the substrate material sequentially with metallic oxide and piezoelectric and/or ferroelectric material and then removing part but not all of the substrate material. The arrays may be used in a variety of applications including liquid delivery and as microelectronic components. A method of generating terahertz emission is also provided.

MICROTUBE ARRAYS

The invention generally relates to microtube arrays, methods for their manufacture, and the use of microtube arrays in a variety of applications including liquid delivery and as microelectronic devices. A further aspect of the invention is directed to the use of microtubes to generate terahertz (THz) emission.

Microtube arrays have been proposed for a number of different applications in the field of liquid delivery, such as the delivery of ink in an inkjet printer head or the delivery of liquid drugs *via* means of an inhaler, for instance. Microtube arrays have also been proposed as 3-dimensional capacitors, in particular in the field of microelectronics, where the need for ever-decreasing component sizes has meant that interest in the development of 3-dimensional capacitors and other 3-dimensional microelectronic components has come to the fore.

However, the development of such components is not straightforward. Indeed, the difficulties encountered in the development of 3-dimensional microelectronic components is illustrated by the fact that the 2006 edition of the International Road Map for Semiconductor Technology provided an expected date of 2010, by which 3-dimensional capacitor structures for ferroelectric random access memories (FRAMs) would be available. However, the 2007 edition of the Road Map pushed back the expected date to 2016. Accordingly, there is a real need for effective and reliable microelectronic components and, in particular, capacitors. Current capacitors tend to comprise a significant proportion of the total area of electronic components available today. Thus, the provision of 3-dimensional capacitors and other components would lead to a significant reduction in the overall size of microelectronic components.

The aforementioned applications are based upon switching of polarisations by electric fields. Accordingly, microtube arrays comprising only ferroelectric or piezoelectric tubes such as those disclosed in GB-A-2414018 and GB-A-2414246 are not sufficient to perform these types of applications, as electrodes are also required to effect switching of the electric field. Work using microtubes comprising gold has been reported in GB-A-2435265 and, more

recently, 3-layer nanotubes based upon palladium, ruthenium, ruthenium oxide ad lanthanum nickelate electrodes have also been investigated. However, there are various drawbacks associated with the precursors necessary to provide these types of electrodes. More specifically, the gold and ruthenium precursors are extremely expensive and not widely available, whilst the polymer-based precursors generally used to provide the palladium electrodes require a time-consuming thermal treatment and result in tubes having granular walls. Another example of the attachment of electrodes to microarrays is reported by Kim *et al* (*Nanoletters*, 2008, 8 (7), pages 1813-1818), who describe PZT nanotube arrays anchored upon a platinised silicon substrate, to which titanium/gold electrodes are attached.

Accordingly, there is a real need for microtube arrays for use in these types of applications, which are easily manufactured from widely available and cheap starting materials but which are, nevertheless, extremely effective in these types of applications.

As mentioned above, the trend in the field of electronics has increasingly been focussed towards higher and higher frequencies in order to provide smaller, lighter and cheaper electronic products. In the last 20 years or so a lot of emphasis has been placed upon gigahertz (GHz) emission. However, more recently, terahertz emission has come to the forefront of this area of research. This is because, with frequencies ranging from approximately 0.1 THz to 10 THz corresponding to the submillimetre wavelength range, even smaller and more light weight devices may be provided.

Nowadays, therefore, there also exists a strong and yet unmet need for high energy ultra-short terahertz pulses for a wide variety of applications including imaging, for instance medical and scientific imaging, security control, quality control and non-linear terahertz spectroscopy to name but a few potential areas of application. In the field of medical imaging and diagnosis, the use of terahertz radiation is particularly attractive as it is non-ionising and is, therefore, not expected to damage tissues and DNA unlike X-rays. Additionally, some frequencies of terahertz radiation can penetrate several millimetres of tissue with low water content, for instance fatty tissue. Also, terahertz radiation can detect differences in water content and density of a tissue. Thus, the use of terahertz

radiation in medical imaging could potentially allow the effective detection of epithelial cancers.

The use of terahertz radiation in scientific analysis such as spectroscopy would provide useful and detailed information in the fields of chemistry and bio-chemistry, for instance. Additionally, the use of terahertz emission in quality control would provide detailed information about imperfections in a wide variety of products, such as pharmaceuticals, foodstuffs, and polymers eg. packaging, to name but a few. Also, as terahertz radiation can penetrate fabrics and plastics, it may find many applications in security screening of, for instance, persons, mail or luggage.

Yet, despite this clear need for sophisticated terahertz emitters and detectors, until recently only free-electron laser sources and femto-second (fs) optical pump systems with ferroelectric lithium niobium oxide ($LiNbO_3$) emitters have been able to generate terahertz pulses that have at least one microjoule of energy. This work is described by Knippels *et al*, in *Phys. Rev. Lett.* 1999, 183, pages 1578-1581 and Yeh *et al.* in *Appl. Phys. Lett.* 2007, 90, entry 171121.

Also, Lee and Norris (*Laser Focus World*, 2005, pages 67-72) describe the generation of terahertz emission *via* the use of poled lithium niobate (PLN) crystals, whilst *Laser Focus World* (2006, page 22-24) reports the generation and detection of terahertz radiation using low temperature indium gallium arsenide (LT-InGaAs) devices. US 7,177,071 describes the generation of terahertz emission using a zincblende-type III-V compound semiconductor crystal. A similar disclosure is found in US-A-2007/0034813.

The lack of development of terahertz emitters and detectors may well be due to two known problems which exist with the construction of ferroelectric-based terahertz emitters and detectors, namely terahertz absorption and the velocity mis-match between terahertz radiation *per se* and the optical signal. These problems have been described in detail by Pradarutti *et al.* in *J. Appl. Phys.* 2007, 102, entry 093105. Hebling *et al* (Optic Express, 2002, 10, pages 1161-1166) and Wang *et al* (Optic Express 2008, 16, pages 6471-6478) have proposed two ways in which to solve the velocity mis-match problem, namely pulse front tilting and domain engineering.

Nevertheless, the velocity mis-match problem is believed to be strongly related to a critical size for ferroelectricity. In more detail, mean-field theory predicts the existence of a critical size equal to the ferroelectric correlation length. This can be interpreted as bulk ferroelectricity suppressed by surface depolarisation energies and implies that the bulk transition has a minimum critical size. An alternative approach is based upon the surface energy, connected with the truncation of the crystal. This predicts different estimates for the dielectric properties and these considerations have been used by Dawber *et al* (*Rev. Mod. Phys.* 2005, 77, pages 1083-1130) to calculate a critical size, which is reported as about 2.5 nm for small spherical particles or thin films of PZT.

There is, therefore, a real need for reliable and effective terahertz emitters and detectors, which are easily and cheaply manufactured. As the terahertz emitters and detectors already known do not encompass the full terahertz wavelength range, there also exists a need to fill the gaps in that range *via* the provision of appropriate devices.

A first aspect of the present invention provides an array of microtubes upwardly extending from a supporting base of substrate material, wherein the tubes comprise at least one concentric layer comprising a metallic oxide and at least one concentric layer comprising a piezoelectric and/or ferroelectric material. A second aspect of the present invention is directed to a method of making the above-described array, in which the walls of pores in the substrate material are lined, sequentially, with a metallic oxide and a piezoelectric and/or ferroelectric material to provide a substrate comprising pores which are lined with concentric layers of the metallic oxide and the piezoelectric and/or ferroelectric material. Part but not all of the substrate material is then removed to provide the array.

Further aspects of the invention are directed to a liquid delivery system comprising an array as defined above in which the piezoelectric and/or ferroelectric material is specifically piezoelectric, and the use of such an array in liquid delivery. A microelectronic device comprising an array as broadly defined above is also provided, as is the use of such an array as a capacitor in a ferroelectric random access memory (FRAM).

A yet further aspect of the present invention is directed to the generation of terahertz emission by subjecting at least one microtube comprising PZT to excitation. The use of such a method in medical imaging, scientific imaging or analysis, quality control and security applications is also provided.

In the context of the present invention, the term "microtube" should be interpreted as referring to tubes which have a diameter in the range of about 10 nm (100 Angstroms) to about 500 nm

The substrate material used in the present invention can be any material in which it is possible to produce pores, and more preferably substantially straight pores, and which can be removed without removal of material deposited in the pores. In the context of the present invention, the term "substantially straight pores" is understood to refer to pores with a ratio of width of the pore at its top to that at its bottom of about 1:1 to about 2:1, the latter of which refers to the case where the pore is narrower at its bottom by about 50%.

Thus, any such materials known in this field would be suitable for this purpose. Preferably, the substrate material is mesoporous. In the context of the present invention, the term "mesoporous" is understood to take its conventional meaning in this field. More specifically, it refers to porous materials in which the pores typically have a diameter of from about 2 nm to about 5 μm. However, porous materials containing pores having diameters outside this range are also suitable for use as the substrate material. For instance, porous materials containing pores with diameters in the range of from about 1 nm to about 10 μm may also be employed. Examples of suitable substrate materials include silicon, alumina, gallium arsenide, indium antimonide and gallium nitride, with silicon and alumina being particularly preferred as they are cheap and readily available materials. Silicon is in fact the most preferred substrate material as there are many known techniques for producing pores in silicon, and more preferably producing substantially straight pores in silicon. Also, silicon is easily removed during the manufacture of the microtube arrays without damaging the deposited tubes.

Known methods for producing the substrate material are described by Ottow *et al* (*Appl. Phys.*, 1996, A63, pages 153-159) and Schilling *et al* (*Appl. Phys. Lett.* 2001, 78 (9), pages 1180-1182). As is known in the art, the substrate

material may typically have a rectangular/orthogonal or hexagonal array of pores. Generally, the pores are substantially cylindrical, preferably substantially parallel and typically extend through all or substantially all of the thickness of the substrate. In addition, the aspect ratio, ie. the ratio of depth to diameter, of the pores is typically high, for instance at least 5, preferably at least 10 and more preferably at least 50. Typically the distance between the pores in the substrate is in the range of about 0.1 to about 10 μm, preferably about 0.5 to about 5 μm and more preferably about 1 μm.

The microtubes comprise at least one concentric layer comprising, consisting essentially of, or consisting of a metallic oxide and at least one concentric layer comprising, consisting essentially of, or consisting of a piezoelectric and/or ferroelectric material. The materials used to form the microtubes may be deposited into the pores of the substrate material using a variety of known techniques. For instance, chemical-solution-deposition (CSD) is a simple, low cost method which may be effectively used to provide microtube arrays according to the present invention. Mist deposition is a form of CSD, which may also be used. Chemical vapour deposition (CVD), metal-organic deposition (MOD) or a combination of the two, namely metal-organic chemical vapour deposition (MOCVD) may also be used to provide microtube arrays according to the present invention. However, these methods are not as preferred as CSD methodologies as they are more expensive and not as straightforward. Standard liquid infiltration and sol-gel techniques may also be used to provide microtube arrays according to the present invention. Decriptions of these known techniques are found in GB-A-2414018 and GB-A-2414246. Kim *et al* in *Nanoletters* describes an integrated sol-gel/spin coating technique which would also be suitable to provide microtube arrays of the invention. Another technique, which has recently been applied to ferroelectric materials, is atomic layer deposition (ALD). This would also be suitable for the preparation of the inventive microtube arrays and is described in detail in Harjuoja *et al* (*Thin Solid Films*, 2006, 496, page 346).

Following deposition of the metallic oxide and or piezoelectric/ferroelectric material, part but not all of the substrate material is removed to provide the array. The known methods for making microtubes described above disclose a

variety of ways in which partial removal of the substrate material may be achieved. Removal can be by any appropriate method, which does not destroy or damage the tubes formed by deposition of the material in the pores. One such suitable method is etching, for instance using acid or alkali. Hydrofluoric acid (HF) is a particularly preferred etchant, in particular when the substrate is silicon, as is described for instance in GB-A-2414246. Removal of part but not all of the substrate material therefore results in the removal of substantially all but not entirely all of the substrate material, such that sufficient substrate material remains to hold the tubes in an array.

The piezoelectric and/or ferroelectric material comprised within the micro arrays of the present invention may be piezoelectric, ferroelectric or both piezoelectric and ferroelectric materials, an example of the latter of which is lead zirconate titanate ($Pb(ZrTi)O_3$;PZT). As is known in the art, all ferroelectric materials are piezoelectric, but not all piezoelectric materials are ferroelectric. A piezoelectric material will expand, contract or bend when an electric field is applied. A ferroelectric material will also expand, contract or bend under application of an electric field but, in addition, has two stable states of bending.

Preferred piezoelectric and/or ferroelectric materials include PZT, lead titanate ($PbTiO_3$), potassium niobate ($KNbO_3$), barium titanate ($BaTiO_3$), barium strontium titanate ($Ba[x]Sr[1-x]TiO_3$; BST), strontium bismuth tantalate ($SrBi_2Ta_2O_9$; SBT), sodium bismuth tantalate ($Na_{½}Bi_{½}TiO_3$), strontium bismuth niobate ($SrBi_2NbTa_2O_9$; SBN), strontium bismuth tantalate niobate ($SrBi_2Ta[2-x]Nb[x]O_9$; SBTN), Aurivilius layer structure oxides of the general formula $(Bi_2O_2)(Sr_{(1-n)}Bi_nO_{(3n+1)})$ in which n is an integer up to 7, and ferroelectric fluorides such as barium fluorides of the general formula $BaMF_4$, wherein M is a metal such as magnesium (Mg), zinc (Zn), cobalt (Co), ion (Fe), manganese (Mn), and nickel (Ni), preferred such barium fluorides being barium zinc fluoride ($BaZnF_4$) and barium magnesium fluoride ($BaMgF_4$).

Given the current environmental concerns associated with the use of materials containing lead, in certain aspects of the present invention the piezoelectric and/or ferroelectric material preferably does not contain lead and is, more preferably, selected from potassium niobate, barium titanate, BST, SBT, sodium bismuth tantalate, SBM, SBTN, the Aurivilius layer structure oxides

described above and the ferroelectric fluorides described above. If desired, a particularly preferred non-lead containing material is SBT.

Alternatively, a particularly preferred piezoelectric and ferroelectric material used in the present invention is PZT. This material is readily available and may be effectively incorporated into microtube arrays according to the present invention using the known techniques described above. PZT is particularly preferred as it is both ferroelectric and piezoelectric, having an abnormally large piezoelectric constant, and it has a perovskite crystal structure, which shows a high potential for piezoelectric device applications due to its high dielectric constant, high Curie temperature, and high breakdown strength. Its range of useful operational temperatures goes well above room temperature and, thus, satisfies military and automotive specifications. Additionally, PZT is chemically robust and rather inert, making it an extremely attractive material for use in a wide variety of applications.

The piezoelectric and/or ferroelectric material used in the present invention may be provided by standard precursors widely known in the art. For instance, for PZT, precursors based upon lead acetate and zirconium- and titanium-iso-propoxyls, such as those commercially available from Kojundo Chemical Corp., may be used.

The metallic oxide incorporated into the microtube arrays of the present invention typically acts as an electrode in the array. A wide variety of metallic oxides are suitable fore this purpose. Examples of particularly suitable metallic oxides include oxides of ruthenium, iridium, strontium, lanthanum, nickel and one or more thereof, with preferred metallic oxides including ruthenium oxide (RuO_2), iridium oxide (IrO_2), strontium ruthenium oxide ($SrRuO_3$) and lanthanum nickel oxide ($LaNiO_3$; LNO). More preferably, the metallic oxide is LNO. LNO is a perovskite-type oxide and is a particularly advantageous substrate as it is a conducting electrode to perovskite ferroelectrics such as PZT. Thus, it is extremely well-matched for inclusion in microtubes with PZT as the piezoelectric and/or ferroelectric material, as effective epitaxial growth of PZT upon the LNO is achieved due to interface lattice matching. Additionally, the use of LNO is desirable as its precursors, examples of which are described in more detail in the accompanying examples, may be readily synthesised using standard sol-gel

techniques and are, thus, widely available. Precursors suitable for the provision of the metallic oxides may be any of those widely known in the art.

Accordingly, it is particularly preferred that the metallic oxide comprises, consists essentially of or consists of LNO while the piezoelectric and/or ferroelectric material comprises, consists essentially of, or consists of PZT.

Sequential lining of the walls of the porous substrate material with the metallic oxide and piezoelectric/ferroelectric materials ultimately provides arrays of microtubes made up of concentric layers of metallic oxide and piezoelectric/ferroelectric materials. Sequential deposition of the metallic oxide and piezoelectric/ferroelectric material results in the outer layers of the microtubes being made up of metallic oxide as this is the material which is initially deposited into the pores of the substrate material.

More preferably, the microtubes comprised within the arrays of the invention contain a first concentric layer of metallic oxide, a second layer of piezoelectric/ferroelectric material and a third concentric layer of metallic oxide, the second concentric layer being positioned between the first and third concentric layers. Even more preferably the microtubes consist essentially of or even more preferably, consist of just these three layers. In such embodiments of the present invention, it is preferred that the first and third concentric layers comprise, consist essentially of or consist of LNO. It is even more preferred that the first and third concentric layers comprise, consist essentially of or consist of LNO, whilst the piezoelectric/ferroelectric middle or second layer comprises, consists essentially of or consists of PZT.

The ends of the microtubes attached to the supporting base may be closed or open. More preferably and depending upon the desired final application of the arrays, a proportion of or substantially all of the ends of the tubes attached to the supporting base are closed, or a proportion of or substantially all of the ends are open. In the context of the present invention, "substantially all" of the ends of the tubes is understood to refer to more than about 50% of the tube ends in the array. More specifically and in the context of open-ended tubes for liquid delivery systems for instance, it simply means that the liquid must be able to flow effectively through the device. In practice, therefore, "substantially all" of the tube ends in the array is desirably greater than

about 50%, more preferably greater than about 70% with, most preferably, greater than about 90% achieving an extremely effective device.

The microtube arrays of the invention are useful in a variety of applications. Firstly, they find application as microfluidic channels, in which the tubes are put into contact with a liquid reservoir and liquid is delivered through the tubes *via* application of a voltage, which can be small for instance approximately 5V, in addition to an applied pressure differential. Thus, the microtube arrays provide effective liquid delivery due to their piezoelectric characteristics. They are, therefore, usefully employed in systems in which a liquid is required to be ejected in the form of very small, ie. micron-sized, droplets of uniform diameter. In the context of the present invention, the term "micron-sized" means that the droplet diameters may vary from a fraction, ie. one third or less, of a micron (micrometre), to several micron, for instance 5 microns.

Liquid delivery systems of particular interest in the present invention are drug delivery systems such as inhalers containing liquid drugs, and cartridges for inkjet printers. For these uses it is of course necessary for the microtubes to be open-ended so that the liquid may pass directly therethrough.

As mentioned above, because the microtube arrays of the invention may comprise ferroelectric materials, they may also be successfully employed in microelectronic devices, for instance as capacitors in FRAMs. For such uses, it is preferred that the ends of the microtubes embedded within the substrate material are closed.

A further use of microtube arrays similar to those described above but which may simply comprise microtubes themselves comprising, consisting essentially or consisting of PZT, is in the generation of terahertz emission. Additionally, individual microtubes comprising, consisting essentially of or consisting of PZT, which are not set within an array, may also be used for this purpose. In more detail, at least one microtube or array comprising PZT microtubes upwardly extending from a supporting base of substrate material, upon excitation, has been found to generate terahertz emission. Any known excitation may be used for this purpose. Particularly suitable sources of excitation include exposure to a laser pulse, for instance by shining an ultra-

short femto-second (fs) laser pulse on to the tube or array. Also suitable for this purpose is the application of a voltage of at least about 5 V and preferably in the range of about 5 V to about 30 V. The use of such voltages as the excitation source is of course significantly cheaper than the use of laser pulsing and, thus, results is significantly cheaper terahertz emitters.

The intense terahertz emission observed to be produced by PZT microtubes and arrays in accordance with the present invention is totally absent flat films or bulk PZT. Accordingly, it is postulated that this effect is due to the nanoscale geometry of the arrays, which contain microtubes of PZT having have a wall thickness on the nanoscale. The wall thickness is typically less than about 250 nm and is preferably from about 20 to about 100 nm, is more preferably from about 30 to about 60 nm, and is most preferably about 40 nm. The wall thickness achieved typically depends upon the viscosity of the precursor material(s) used to form the microtubes. Thicker tubes are more robust but require higher voltage for excitation and result in less dense arrays. Thinner tubes are more fragile. Thus, wall thicknesses of approximately 30 to 50 nm and, more preferably, about 40 nm are particularly desirable.

The terahertz radiation emitted by the microtube or array is typically emitted within approximately 0.2 picoseconds (ps), and the spectrum so-obtained preferably exhibits a broad peak of from about 0.3 to about 10 THz and more preferably from about 2 to about 8 THz. This is a gap in the frequency spectrum of semiconductor terahertz devices, such as known zinc telluride devices, and it is an order of magnitude higher than the frequency peak observed for the well-documented p-type indium arsenide (p-InAs) systems, due to the abnormally large carrier concentration gradient in PZT. It is thought that the inferred mechanism by which the terahertz emission is generated is optical rectification within a surface accumulation layer (as described by Chuang *et al.*, in *Phys. Rev. Lett.*, 1992, 68, pages 102-105), rather than being due to the Dember effect (as described by Dekorsy *et al.*, in *Phys. Rev.* B, 1996, 53, pages 4005-4014).

In addition, an electron paramagnetic resonance (EPR) signal has been observed for the microtubes, which are used to achieve THz emission according to the present invention. It has been established that the EPR signal comes

from oxygen trapped within the PZT microtubes. This conclusion was reached by quantitative comparison of these EPR results with those reported by Simon *et al.* (J. Chem. Soc., *Faraday Trans.*, 1994, 90(18), pages 2663-2670). There is a strong quantitative similarity between the oxygen centre described by Simon *et al.*, which is unambiguously identified as arising from oxygen trapped in the cavities of their samples, and the EPR signals observed for the tubes described herein.

The method of generating terahertz emission according to the present invention is applicable to a wide variety of applications and, in particular, imaging applications. It is preferably applied in medical imaging, for instance for the purposes of diagnosis, scientific imaging such as spectroscopic analysis, quality control of a wide variety of products including but not limited to pharmaceuticals, foodstuffs, polymeric materials in particular films and the like, and it is also applicable in a wide variety of security applications as terahertz radiation can penetrate fabrics and plastics. Thus, the method of generating terahertz emission according to the present invention finds utility in security applications including but not limited to security screening of persons, mail or luggage, for example.

The present invention will be now be described with reference to the following examples and figures:

Figure 1 is (a) a schematic representation of apparatus used to perform chemical-solution-deposition (CSD) to provide a microtube array of the invention and (b) a sample array structure;

Figures 2 (a) and (a') are scanning electron images of LNO microtube arrays;

Figure 3 is a schematic representation of concentric microtubes of LNO and PZT layers embedded within a silicon substrate;

Figures 4 (b) and (b') are scanning electron images of LNO-PZT-LNO microtube arrays;

Figure 5 shows Energy Dispersive X-ray spectroscopy (EDX) elemental mapping of LNO-PZT microtubes and part of the tube wall. The horizontal dashed line is a guide for the eye;

Figure 6 shows X-ray Diffraction (XRD) spectra of PZT, LNO and LNO plus PZT microtube arrays protruding from an Si matrix;

Figure 7 shows P-E hysteresis loops under different applied voltages for an approximately 100 nm PZT film deposited upon (a) an LNO thin film and (b) platinum-coated silica (SiO_2) flat substrates. The top electrodes for both cases are platinum made by sputtering through a mesh mask;

Figure 8 illustrates switching of an individual vertically-aligned PZT tube using piezoresponse force microscopy (PFM);

Figures 9 (a), (b) and (c) are scanning electron microscopy images of PZT nanotubes, in which (a) and (b) are tilted views and (c) is a top view;

Figure 10 is a schematic representation of apparatus used to produce terahertz emission using laser excitation;

Figures 11 (a) and (b) show the wave form and spectra respectively of a terahertz pulse generated from a PZT microtube array; and

Figure 12 illustrates the temperature dependence of terahertz reflectivity from a silicon surface attached to PZT nanotubes and from an empty porous silicon substrate;

Figure 13 shows EPR signals obtained from PZT microtubes.

Example 1: Preparation of LNO-PZT-LNO Microtube Array using Liquid Infiltration Techniques

Porous Si templates were fabricated by etching of n-type phosphorous doped Si wafer. The doping density is dependent on the desired pore size. For a sample with 2 μm pore diameter, the resistivity is 5 Ω·cm, which corresponds to a doping density of $1x10^{15}$ cm^{-3}. The pore diameter can be tuned between 500 nanometer (nm) to 10 micrometer (μm) by adjusting the doping and etching current density. Accordingly the interpore distance can also be varied. The pore depth depends linearly on the etching time. Both 50 and 100 μm deep pores have been used.

PZT Precursor Solution

A commercially available PZT metal-organic-decomposition (MOD) precursor was obtained from Kojundo Chemical Corp. The composition has a ratio of PB/ZR/Ti of 1.1/0.4/0.6. This represents a 10% excess of lead due to the fact that some of the lead will evaporate on heating. The initial composition was 17 % PZT, which was then diluted to 4 % PZT using methyl ethyl ketone.

Preparation of LNO Precursor Solution

The $LaNiO_3$ sol precursor was synthesized from nickel acetate [$Ni(CH_3COO)_2 \cdot 4H_2O$] and lanthanum nitrate [$La(NO_3)_3$] as follows. Nickel acetate was dissolved in acetic acid and an equimolar amount of lanthanum nitrate was dissolved in distilled water, both at room temperature. The two solutions were then mixed together with constant stirring. Then, dimethylformamide was added to the solution in order to avoid crack formation during heating. The final concentration of the precursor solution was 0.3 M in La. The resulting solution was green in colour.

Deposition of LNO and PZT on to Substrate Material

The substrates used were 1.5 x 1.5 cm^2 in dimension. The solution of LNO or PZT obtained as described above was contained in a glass bottle (2 cm in diameter). The porous Si template was immersed into the solution for 3 mins. A slight vacuum was applied above the solution by covering the openings with a shower-head and an O-ring in between, as illustrated in Figure 1.

Deposition may also be made without vacuum, in which case the substrates are immersed in the solution (LNO or PZT) for about 30 mins.

The sample was then dried at 80°C on a hotplate for about 10 mins, then heated at 300°C for another 10 mins, followed by annealing in a resistant furnace at 700°C (in case of LNO) or 650°C (in case of PZT) for 20 mins *via* insertion of the samples into the pre-heated tube. The whole process is repeated twice for both LNO and PZT.

Alternatively, the precursor(s) are effectively deposited on to the porous Si templates using mist deposition, in particular *via* means of a Samco Co. mist deposition machine, at about 0.5 atm of air. The resulting sample is then dried and heated to about 650 °C in a rapid thermal annealer for about 90 seconds. Oven annealing for 30 mins has been found to be equally effective to the use of a rapid thermal annealer.

Following deposition of the LNO and PZT on to the Si substrate, part of the substrate was then etched away using dilute alkaline aqueous potassium hydroxide solution. However, it has been found that acidic etchants may also be used, such as dilute hydrofluoric acid and dilute nitric acid.

Arrays containing only LNO tubes were also manufactured by this method.

In order to scale-up this procedure, larger solution containers and specially-designed evaculating apparatus are needed. For example, Figure 1 illustrates a proposed apparatus for use with wafer substrates. Note that 10 cm wafer porous

silicon substrates are also commercially available and could be used in the present invention.

Characteristics of Tubes and Arrays

The LNO tubes so-manufactured are continuous and robust, which is beneficial for electric contacting purposes. These superior physical characteristics are illustrated by Figure 2.

The three layer LNO-PZT-LNO tubes represented by Figure 3 have a total wall thickness of approximately 200 nm and a clean hollow interior after repetitious infiltrations, as shown in Figure 4. The tube wall thickness has a reasonable homogeneity. Overall the tubes have a test-tube like morphology as a replica of the blind pores of the Si templates. However, 100 μm long tubes with both ends open have also been made using membrane Si templates with see-through channels.

The tubes have been round to be perovskites having a polycrystalline wall. This was confirmed by X-ray diffraction data. The elements La, Ni, Pb, Ti, Zr, and O were verified using transmission-electron microscopy, which reveals a spatial mapping of the selected elements, as shown by the EDX images in Figure 5. The LNO layer is quite homogeneous whereas the PZT layer is somewhat non-uniform (see top part of Figure 5). The mapping images recorded from the edge of a tube (see bottom of Figure 5) shows that Si is on the outside, then La (and Ni) inside in a distinct band, followed by the diffuse PZT inside the LNO. This is consistent with the trilayer structure in the scheme in Fig. 1. It is noted that a Si layer exists on the outer surface of the tube. The Si might be due to diffusion from the template during annealing, as also found in the case of carbon nanotube template (S. Kawasaki *et al.*, Appl. Phys. Lett., 2008, 92, entry 053109), but a more likely origin is a SiO_x layer which formed by oxidation and was not removed by KOH.

The XRD spectra of the microtube arrays, measured after partial etching of the Si, are shown in Figure 6. From this, it is clear that all the tubes are crystallized. All the peaks can be indexed to perovskite PZT after the annealing at 650 °C. This is in contrast to Bharadwaja's case, in which a 700 °C annealing temperature was needed to obtain a perovskite phase (see S. S. N. Bharadwaja *et al.*, J. Am. Ceram. Soc., 2006, 89, page 2695). This could be due to the difference in the precursor types: Here, a MOD precursor has been used, whereas Bharadwaja *et al.* used a normal sol precursor. The peaks of LNO tubes are also consistent with literature. The peaks for the LNO+PZT tubes can be assigned according to those of the

constituents. TEM investigations reveal that the tube wall is polycrystalline containing < 50 nm sized crystallites.

The P-E and/or C-V measurement of an individual microtube have also been performed. In Figure 7, hysteresis loop of a control sample, which is PZT film of similar thickness to that of the tube wall deposited on a LNO film, is shown. The resistivity of the LNO film was estimated to be about two orders higher than Pt based on four-point measurement. The remanent polarization Pr, 15 $\mu C/cm^2$ under an applied voltage of 14 V, is lower than that of PZT film of the same thickness on Pt electrode, 22 $\mu C/cm^2$. However, their coercive fields are very close, being 200 kV/cm. The rectangularity of hysteresis loop of the PZT/LNO is somewhat worse than that of PZT/Pt. This might be related to the surface roughness of the LNO film due to its poor wettabilty on SiO_2.

The PZT tubes have also shown piezoresponse hysteresis as determined by piezoresponse force microscopy (see Figure 8). Polarization-electric field measurement of a control sample also showed a clear hysteresis loop. A remanent polarization of P_r = 15 $\mu C/cm^2$ under an applied voltage of 14 V was obtained.

The LNO and PZT sol precursors enter the pores due to a capillary effect. A similar three-layer film may also be formed on the surface of the Si substrate. Such trilayers may be utilized for electrically contacting the tubes to activate the piezoelectricity, for example for use in liquid delivery systems, or to switch the polarization, for 3-D capacitors. Individual addressing may be realised by isolating the tubes using lithography plus etching techniques, or using focussed ion beam techniques. However it has been found that, if the substrate surface is dirty or oxidized into silica (SiO_2), it becomes hydrophobic so that the LNO, which is water-based sol solution, wets the substrate surface only poorly. This results in the surface layer thickness being too thin, e.g. around 10 nm or less, to be conducting (LNO) or insulating (PZT). Thus, it is preferred that the Si substrates should be made hydrophilic by chemically treating in a conventional manner to remove the organic absorbents and oxides.

Example 2: Generation of Terahertz Emission and Reflectivity using Arrays of PZT Microtubes

Fabrication of Microtube Arrays

PZT tubes were fabricated by solution infiltration of porous Si templates using 4 wt% metalorganic decomposition (MOD)-type $Pb(Zr_{0.4}Ti_{0.6})O_3$ precursor. The Si

used for fabrication of the porous template was doped with phosphorus giving a resistivity of 10 Ω·cm. The pores were ordered in a hexagonal array, with a 1 μm diameter, 2 μm inter-pore separation, and 18 μm depth as measured by scanning electron microscopy (SEM). After infiltration, the sample was dried at 80 °C for about 30 mins, then heated at 300 °C for another 30 mins, followed by annealing in a furnace at 650 °C for 20 mins. Finally, the PZT tube arrays were partially exposed from the Si matrix by etching the Si matrix in a 30 wt% KOH solution at room temperature for 1 hr. The tubes obtained had a wall thickness of 45±5 nm as measured by SEM. The exposed part of the tubes was 3 m long, while the remaining part, about 15 m long, was embedded within the Si. Figure 9 shows the representative scanning electron microscopy images of the PZT tube array.

Terahertz Emission

Figure 10 schematically shows an experimental set-up for THz emission laser excitation from surface experiment: A fiber-optic laser delivered pulses of 70 femtoseconds' (fs) duration at a wavelength of 800 nm with a 90 MHz repetition rate. The pump beam was incident at 45° to the sample surface. The average pump laser power was ~ 40 mW. THz radiation was focused by means of a Si lens and collected by a photoconductive detector. The detector was fabricated from the layer of GaAs grown by molecular beam epitaxy at low (~250°C) substrate temperature.

Figure 11 shows the time-domain waveforms measured on a PZT nanotube sample (sample 7a) and its corresponding fast-Fourier transform spectra. The traces labeled 5a are for an identical mesoporous Si substrate with no PZT and exhibit only noise. Similar to other ferroelectrics, the main THz generation mechanism in PZT nanotubes is optical rectification.

Terahertz Reflectivity

Since the Si substrates were n-type doped (with a doping density of 5×10^{15} cm^{-3}), they were opaque in THz range. Therefore, THz reflectivity measurements were performed with a THz spectrometer based on an optically pumped THz laser (obtained from Edinburgh Instruments). The THz detector was a highly sensitive pyroelectric.

THz reflectivity was measured from an empty porous Si surface and from the Si surface with protruding PZT nanotubes at different frequencies in the 0.5-6.5 THz range and the temperature range of 4-300 K. In both cases, the THz reflectivity increased on cooling as illustrated in Figure 10. This increase is mainly due to the

increase of the Si conductivity. A similar increase attributed to carrier mobility was reported for p-InAs by Mendis *et al* (J. Appl. Phys, 2005, 98, entry 126104).

Analysis and Interpretation of Results

Terahertz emission in semiconductors has been carefully studied in the past in a variety of semiconductors. Following the 1992 report from Zhang and Auston , J. Appl. Phys, 1992, 71, pages 326-338), there were several models proposed, basically involving optical rectification· Chuang *et* al, Phys, Rev. Lett. 1992, 68, pages 102-105) or the optical Dember effect (Dekorsky *et al*, Phys, Rev. B 1996, 53, pages 4005-4014). In some cases the effect is thought to be due to optical rectification, and, in particular, the response of the gradient in carriers produced within the surface accumulation layer in p-InAs is moot. It is possibly due to carrier gradients and optical rectification or possibly due to the Dember effect. However, for wide-bandgap materials such as PZT (E_g = 3.6 eV), the photo-Dember effect should be negligible, because the absorption depth is relatively deep. In the present study example, the THz spectrum produced is similar to that known in p-InAs [100] but shifted to a frequency range about one order of magnitude higher, which could be useful for agile frequency devices. This increase in frequency is thought to arise from the abnormally large carrier concentration gradient in PZT, which decreases from 3 x 10^{20} cm^{-3} at the surface to 5 x 10^{18} cm^{-3} in the interior of the film at only 20 nm deep. This increase is due to oxygen vacancy concentration and is orders of magnitude greater than in any conventional III-V or II-VI semiconductor. In addition, the carrier mobility in PZT is much lower, i.e. of the order of 10^{-6} $cm^2/V.s$, which further increases the carrier concentration gradient near the surface when subjected to fs laser pulses, in comparison with InAs, as reported by Goldman *et al* (J. Appl. Phys, 1978, 49, pages 2849-2854).

EPR of PZT nanotubes

Because of the interesting THz properties of the PZT nanotubes and their dependence upon surfaces and surface-to-volume ratios, the local structure of these nanotubes was investigated by electron paramagnetic resonance (EPR).

Two different samples were studied. The first one consisted of PZT nanotubes together with the Si substrate (see Figure 9). The second one was the same sample but the PZT nanotubes were brushed off by polishing so that no PZT tubes protrude the Si substrate. The corresponding X-band EPR spectra are shown in Figure 13. As it can be seen there is no EPR spectrum in the pure substrate whereas a rather

strong one in the nanotube sample. The spectrum from nanotubes is asymmetric (Figure 13) and extends from 1,500 Gauss to 12,500 Gauss. It has a maximum around 12,000 Gauss demonstrating a rather small g factor ($g \approx 0.58$). The spectrum is unobservable at high temperatures but is strong at low temperatures.

As a control experiment, pure SiO_2 tubes without PZT, which was obtained by thermal oxidation of a porous Si substrate at 1200 °C plus KOH etching, was also studied. No EPR signal was observed.

It is known that oxides have a lot of oxygen vacancies randomly distributed in the host lattice (Maiwald *et al.*, *Europhys. Lett.*, 2003, *64*, pages 776-778, and Laguta *et al., J. Appl. Phys.*, 2003, *93*, pages 6056-6064). This may lead to a random distribution of cations with different valency. Some of them can be magnetic or non-magnetic depending on whether their ground state spin is zero or non-zero. An O^- ion in an oxide perovskite has a singly degenerate p_{σ} and double degenerate p_{π} orbitals. An acceptor at the A-site of ABO_3 perovskites is surrounded by twelve O^{2-} ions and at the B-site by six such ions. The point symmetry of the cluster of oxygen ions is broken by the localization of the hole at one of the equivalent O^{2-} ions of the cluster. This corresponds to the formation of a small hole polaron bound to an acceptor. The Jahn-Teller interaction lifts the two-state orbital degeneracy supporting the hole polarization. The EPR spectrum is thus due to "Jahn-Teller polarons" (see Maiwald *supra*, and Vikhnin *et al.*, *Sol. Stat. Commun.* 200, *113*, pages 455-460).

The breaking of the local symmetry leads to the fact that one of two degenerate p_{π} orbitals has become the ground state. The splitting of the ground state is due to spin-orbit coupling which acts as a perturbation leading to "negative" deviations of the g-values from the free-electron value, $g_s = 2$. This is true as the g-shift Δg is proportional to

$$\Delta g \propto \lambda / \Delta E \qquad \text{(Equation 1)}$$

Here ΔE is the difference between the ground and the excited state energy and lambda is the spin-orbit perturbation.

The Zeeman Hamiltonian now is:

$$H_z = \mu_B \vec{B}_0 (g_L \vec{L} + g_s \vec{S}) \qquad \text{(Equation 2)}$$

To Equation 2 one should add the local magnetic field Hamiltonian. It should be noted that for a free O^{-2} ion the orbital g-value equals to 1, $g_L = 1$. This, together with a dynamic Jahn-Teller interaction[30] explains the "negative" g-shift.

There is a significant difference[a] between the EPR spectra of electronic centers near the surface and in the bulk. In analogy to planar films, centers which are more that 1000 nm away from the surface, i. e. thick films, should exhibit bulk properties. Those however which are closer to the surface should show characteristic surface properties (thin films). Because of the lowering of the symmetry near the surface the number of EPR lines is expected to increase. Another difference is the dependence of the resonance line positions on the angle □ between the direction of the magnetic field and the normal to the surface. The shift of the g-value, as given by Equation 1, can be reformulated in the case of a planar thin film as

$$\Delta g = -C \sin^2 \theta \qquad \text{(Equation 3)}$$

The lines of the surface centers are strongly shifted to large magnetic fields, i.e. lower g-values. The shift is zero for the magnetic field parallel to the normal of the surface. It is maximal for the magnetic field being in the plane of the surface.

As PZT is a non-magnetic material, the EPR signal shown in Figure 13 is most likely due to O^- holes similar as seen in $KTaO_3$ (see Maiwald *supra*). In addition, such O^- signal does comes from the PZT tube, rather than from a thin SiO_2 layer on top of the tube surface, since no peak was observed from the sample containing only pure SiO_2 tubes.

Since relatively thick films are dealt with here, the spectra are bulk-like and the surface spectra are nearly negligible. The spectrum is a frequency distribution, as seen from relaxation measurements. The negative g-shift further demonstrates that Jahn-Teller small polarons formed by O^{2-} holes bound to an acceptor are probably present, but definitive characterization of the oxygen species is incomplete, and it is not absolutely certain that it is O^{2-}.

CLAIMS

1. An array of microtubes upwardly extending from a supporting base of substrate material, wherein the tubes comprise at least one concentric layer comprising a metallic oxide and at least one concentric layer comprising a piezoelectric and/or ferroelectric material.

2. An array according to claim 1, wherein the metallic oxide is selected from ruthenium oxide, iridium oxide, strontium ruthenium oxide and lanthanum nickel oxide (LNO).

3. An array according to claim 2, wherein the metallic oxide is LNO.

4. An array according to any preceding claim, wherein the piezoelectric and/or ferroelectric material is selected from lead zirconate titanate (PZT), lead titanate, potassium niobate, barium titanate, barium strontium titanate (BST), strontium bismuth tantalate (SBT), strontium bismuth niobate (SBN), strontium bismuth tantalate niobate (SBTN), Aurivilius layer structure oxides of the general formula $(Bi_2O_2)(Sr_{(1-n)}Bi_nO_{(3n+1)})$ wherein n is an integer selected from 1 to 7, and barium fluorides of the formula $BaMF_4$ wherein M is a metal selected from Mg, Zn, Co, Fe, Mn, and Ni.

5. An array according to claim 4, wherein the piezoelectric and/or ferroelectric material does not contain lead.

6. An array according to claim 4, wherein the piezoelectric and/or ferroelectric material is PZT.

7. An array according to any preceding claim, wherein the substrate material is mesoporous.

8. An array according to claim 7, wherein the mesoporous substrate material is selected from silicon, alumina, gallium arsenide, indium antimonide and gallium nitride.

9. An array according to claim 8, wherein the substrate material is silicon or alumina.

10. An array according to any preceding claim comprising a first concentric layer of metallic oxide, a second concentric layer of piezoelectric and/or ferroelectric material and a third concentric layer of metallic oxide, wherein the second concentric layer is positioned between the first and third concentric layers.

11. An array according to claim 10, wherein the first and third concentric layers comprise LNO.

12. An array according to claim 11, wherein the piezoelectric and/or ferroelectric material is PZT.

13. An array according to any preceding claim, wherein substantially all of the ends of the tubes attached to the supporting base are closed.

14. An array according to any of claims 1 to 12, wherein substantially all of the ends of the tubes attached to the supporting base are open.

15. An array according to claim 14, wherein the piezoelectric and/or ferroelectric material is piezoelectric.

16. A method of making an array of microtubes upwardly extending from a base of substrate material, the method comprising lining the walls of pores in the substrate material sequentially with a metallic oxide and a piezoelectric and/or ferroelectric material to provide a substrate comprising pores which are lined with concentric layers of the metallic

oxide and the piezoelectric and/or ferroelectric material, and removing part but not all of the substrate material to provide the array.

17. A method according to claim 16, wherein the array is as defined in any of claims 1 to 15.

18. A liquid delivery system comprising an array as defined in claim 15.

19. A liquid delivery system according to claim 18, which is a drug delivery system.

20. A liquid delivery system according to claim 18, which is a cartridge for an inkjet printer.

21. Use of an array as defined in claim 15 for liquid delivery.

22. Use according to claim 21, wherein the liquid delivery is selected from drug delivery and inkjet printing.

23. A microelectronic device comprising an array as defined in any of claims 1 to 15.

24. A microelectronic device according to claim 23, in which the array is a capacitor in a ferroelectric random access memory (FRAM).

25. Use of an array as defined in any of claims 1 to 15 as a capacitor for a FRAM.

26. A microelectronic device according to claim 23 or claim 24 or a use according to claim 25, wherein the array is as defined in claim 13.

27. A method of generating terahertz emission comprising subjecting at least one microtube comprising lead zirconate titanate (PZT) to excitation.

28. A method according to claim 27, wherein the at least one microtube is comprised within an array of microtubes comprising PZT upwardly extending from a supporting base of substrate material.

29. A method according to claim 27 or claim 28, wherein excitation of the microtube(s) is achieved by application of a voltage across the wall(s) of the microtube(s).

30. A method according to claim 29, wherein the voltage is in the range of about 5 V to about 30 V.

31. A method according to claim 27 or claim 28, wherein excitation of the microtube(s) is achieved by application of a laser pulse.

32. A method according to any of claims 27 to 31, wherein the terahertz emission has a frequency in the range of about 0.3 THz to about 10 THz.

33. A method according to any of claims 27 to 32, wherein the thickness of the walls of the microtubes is in the range of about 20 to about 100 nm, preferably from about 30 to about 60 nm, and is more preferably about 40 nm.

34. Use of a method according to any of claims 27 to 33 in medical imaging, scientific imaging, quality control or security applications.

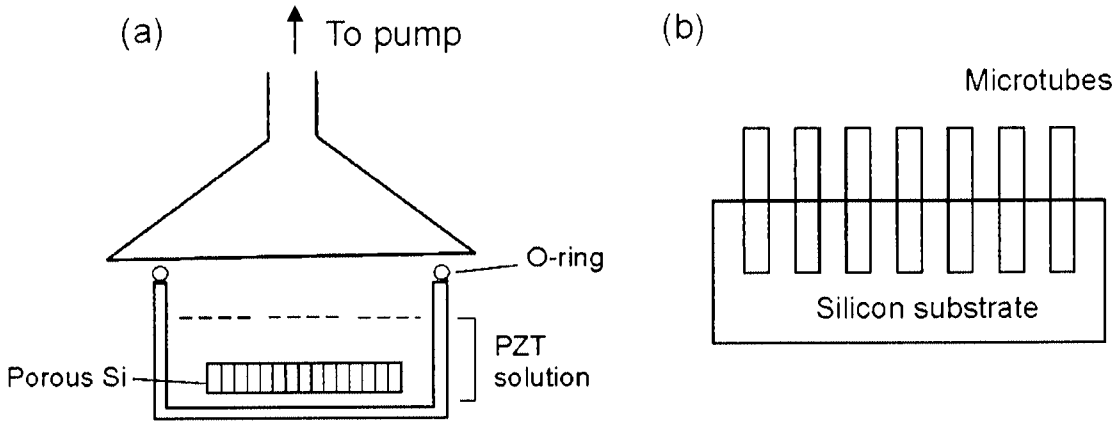
(a)
To pump
O-ring
PZT
solution
Porous Si
(b)
Microtubes
Silicon substrate

Figure 1

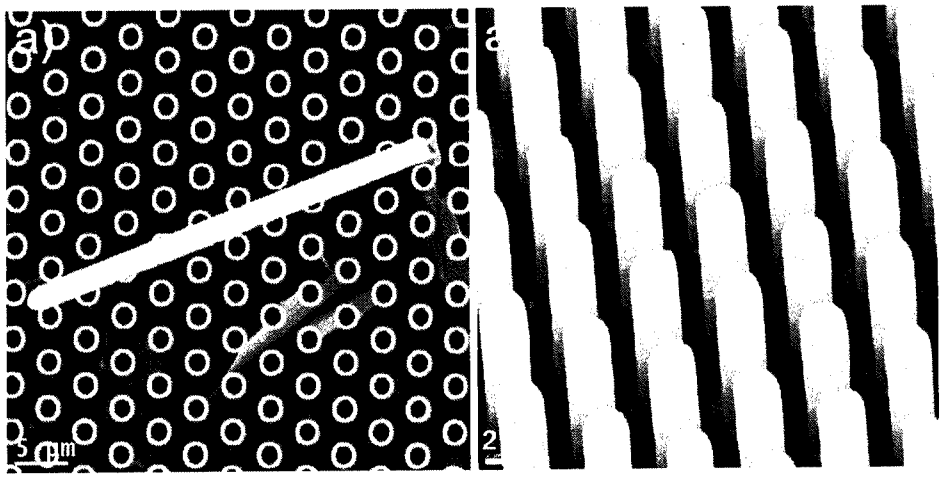

Figure 2

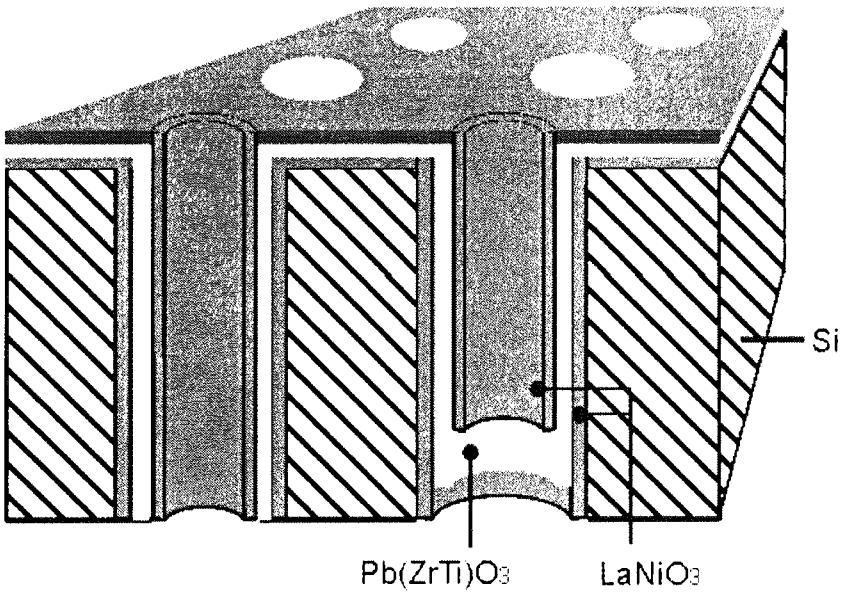

Figure 3

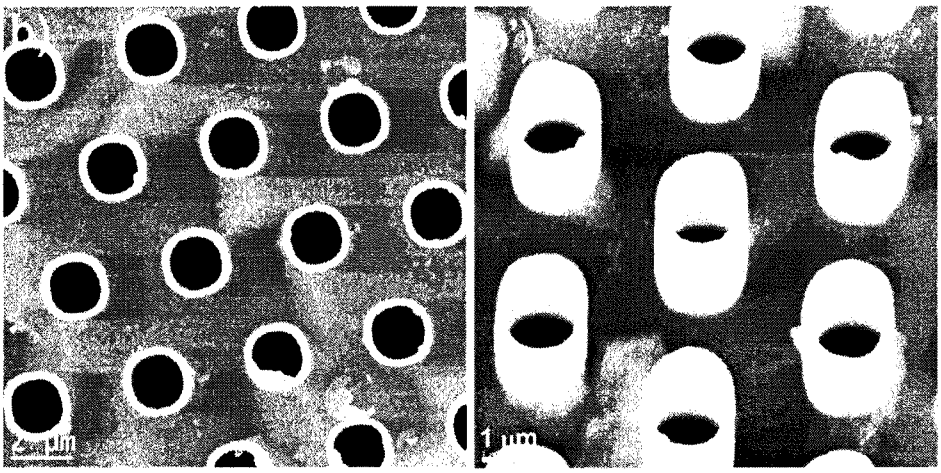

Figure 4

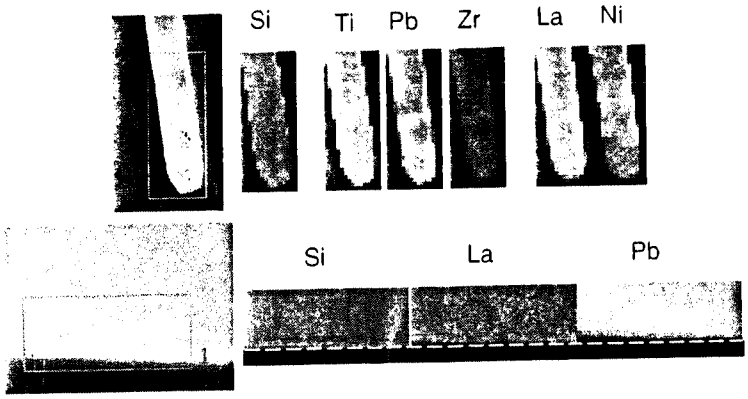

Figure 5

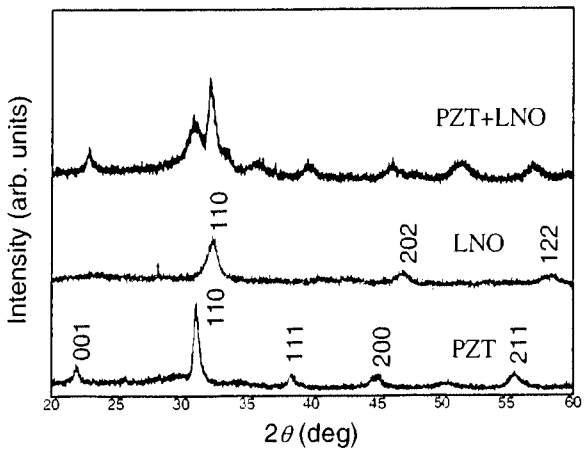

Figure 6

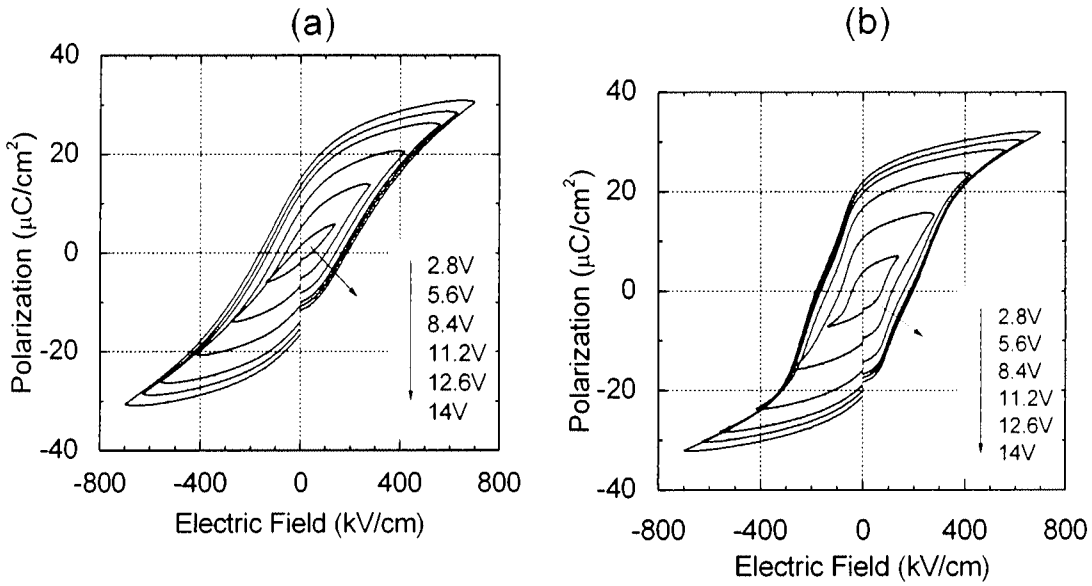

Figure 7

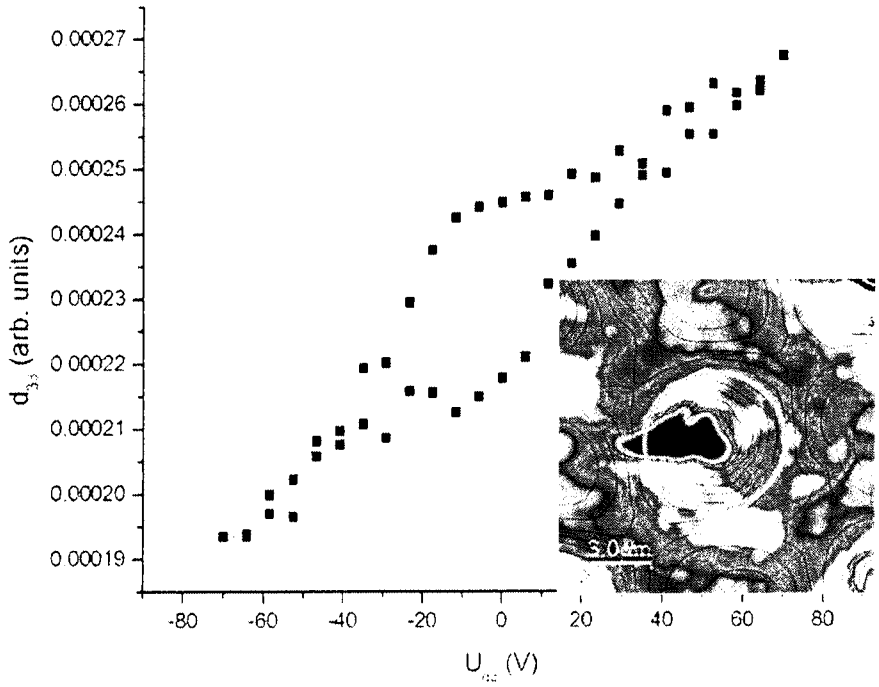

Figure 8

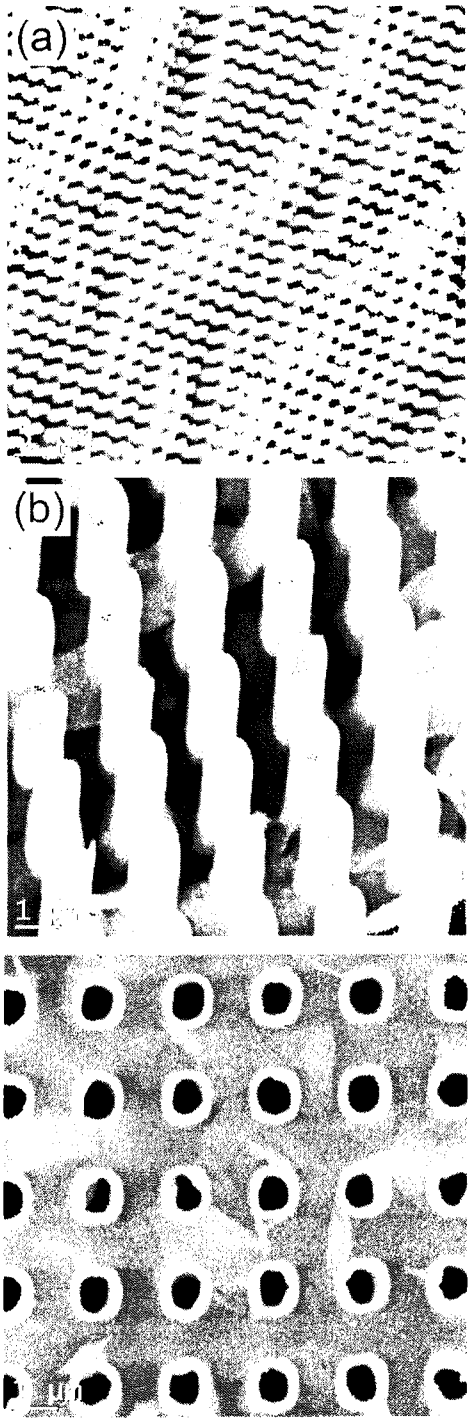

Figure 9

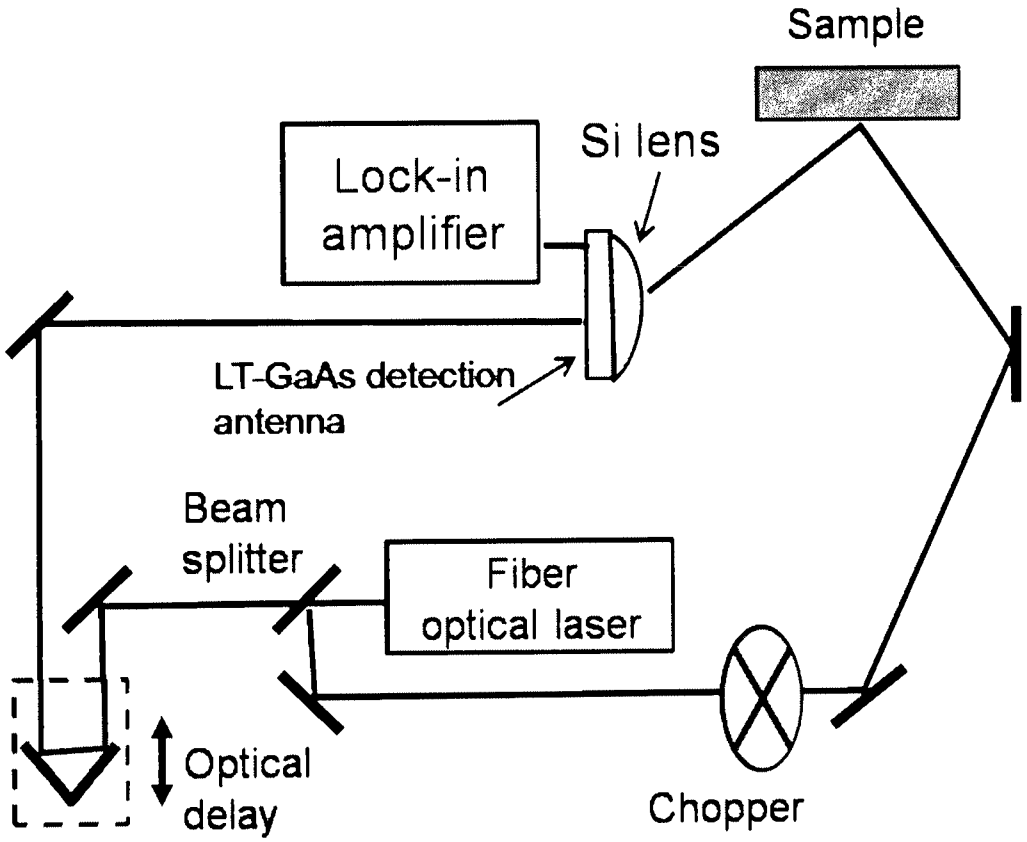

Figure 10

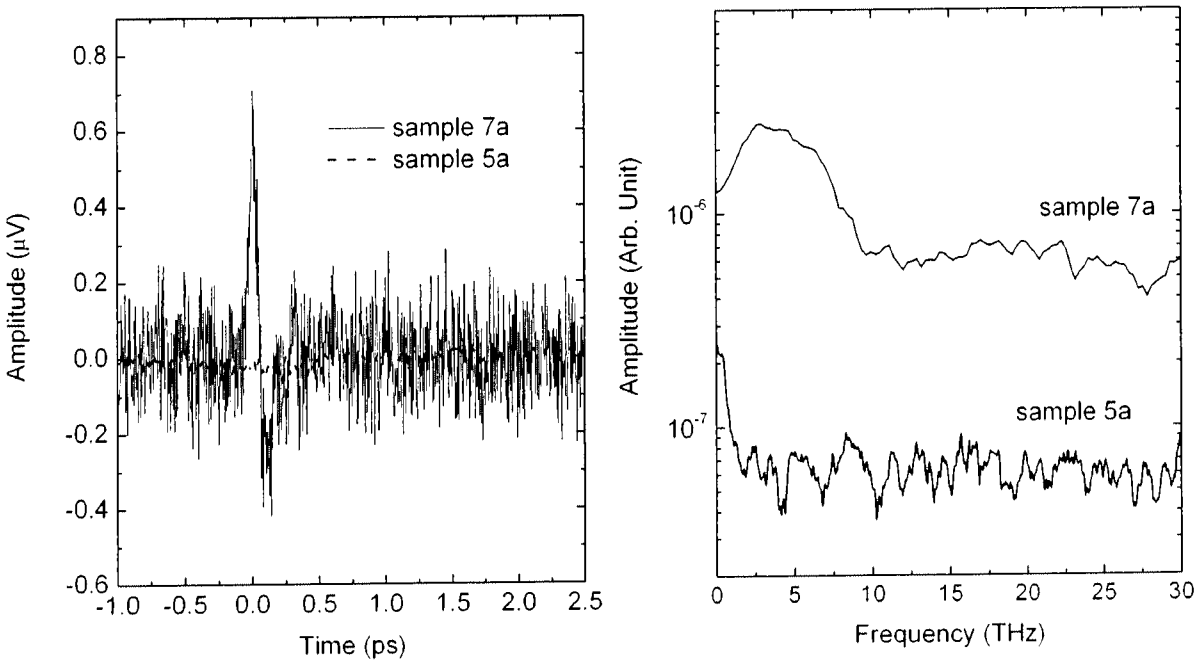

Figure 11

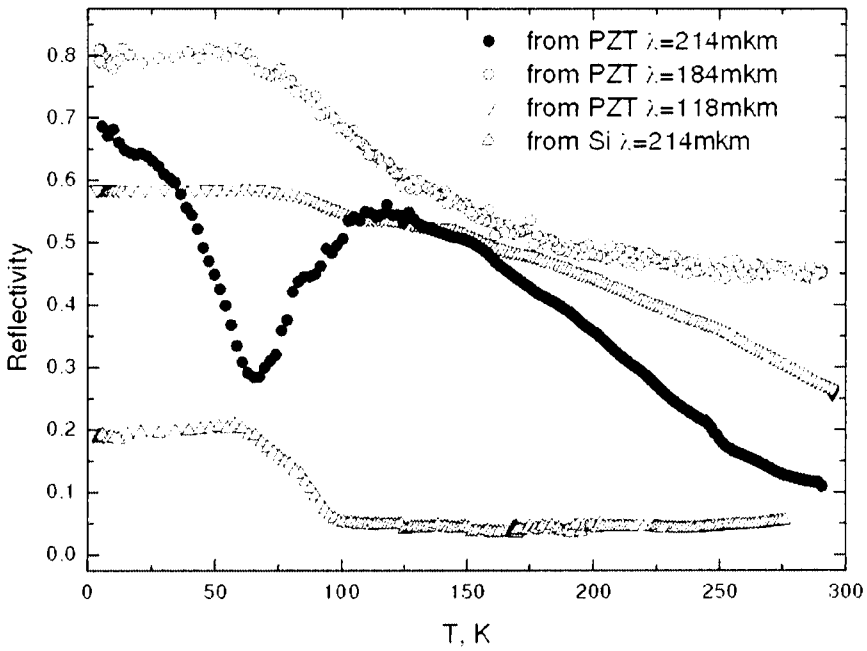

Figure 12

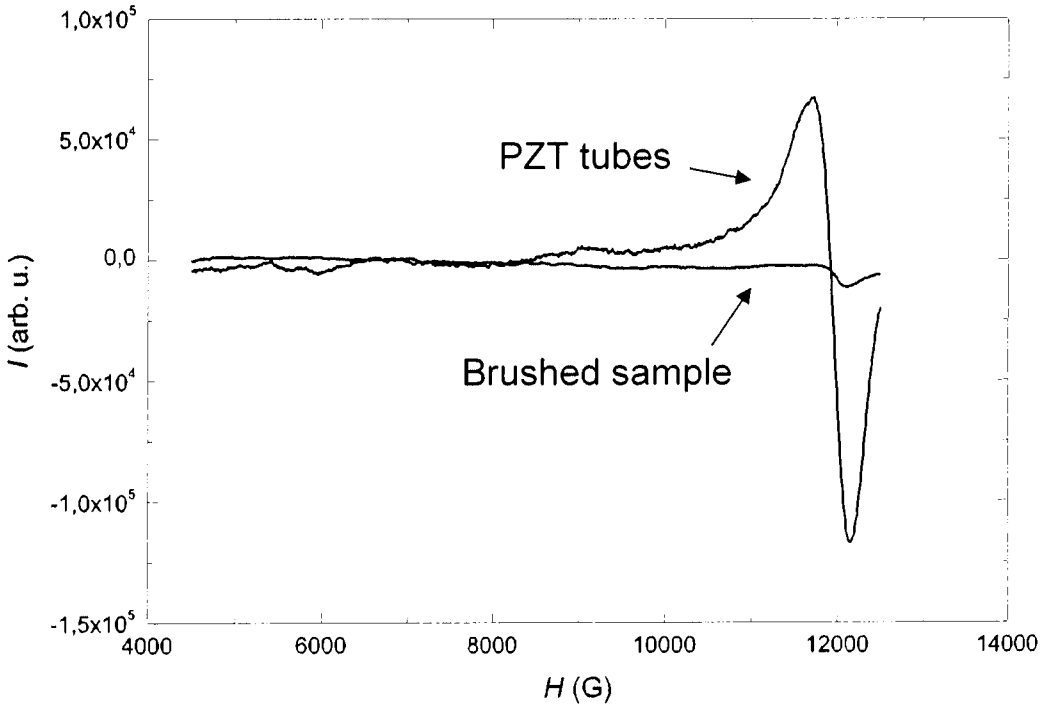

Figure 13